ISSN 1318-0010
KZLTET 31(6)507(1997)

ULTRA THIN DEPOSITED AND SEGREGATED FILMS

ULTRA TANKE NANESENE IN SEGREGIRANE PLASTI

MONIKA JENKO

Institute of Metals and Technology, Lepi pot 11, 1000 Ljubljana, Slovenia

Prejem rokopisa - received: 1997-10-01; sprejem za objavo - accepted for publication: 1997-10-21

Dedicated to Prof. Jože Gasperič at the occasion of his 65th birthday

Research, development and use of vacuum thin films started at the Institute for Electronics and Vacuum Techniques, IEVT, Ljubljana after its foundation around 1950. With the development of the miniature thin film potentiometers and thin films resistors of high stability at IEVT the first production of thin film electronic components in former Yugoslavia was established. The technology was successfully transferred to Slovenian foreign factory in Cormons Italy where Slovenian minority is living. At the same time the high tech research and development of the second and third generation image intensifier tubes was started. Prof. Dr. Jože Gasperič was one of the leading scientists investigating the sputtered cermet thin films in his BS and Ph.D. works. His findings are basic for understanding the mechanism of growth of thin sputtered cermet films. In the middle of eighties an experimental ultra high vacuum, UHV, system equipped with Auger spectrometer, was built at IEVT and the investigation of physical and chemical processes of ultra thin oxide film growth on the surface of liquid indium and indium alloys in situ was achieved for the first time. The experimental method based on Auger Electron Spectroscopy for in situ investigation of the initial phase of the ultra thin oxide film growth on liquid indium, was developed at the institute. The modified experimental method was also used for the study of ultra thin segregated Sb, Sn or Se films on the surface of FeSiC alloy, microalloyed by Sb, Sn or Se. The investigation of ultra thin Sn, Sb or Se films on well defined Fe surfaces is the topic of our present research which is close connected with the purchase of new AES/XPS instrument with the very high spatial resolution. The results of investigations of ultra thin oxide films on the liquid indium and InSn alloy as well as Sb and Sn ultra thin film growth on the surface of FeSiC alloy were presented.

Key words: ultra thin films, deposited films, segregated films, surface segregation, oxidation, dissociation

Prve raziskave, razvoj in uporaba vakuumskih tankih plasti so se začele na Inštitutu za elektroniko in vakuumsko tehniko v Ljubljani takoj po ustanovitvi, okrog leta 1950. Z razvojem miniaturnega tankoplastnega potenciometra MP in stabilnih tankoplastnih miniaturnih uporov se je pričela na IEVT tudi prva proizvodnja tankoplastnih elektronskih komponent v takratni Jugoslaviji. Tehnologija izdelave MP je bila uspešno prenesena v novo ustanovljeno slovensko zamejsko tovarno v Krminu v Italiji. Obenem pa so se vršile raziskave in razvoj specialnih fotoelektronk, Sb fotokatod druge in tretje generacije za slikovne ojačevalnike z bližinskim prenosom slike, ki je predstavljal "high-tech" v svetovnem merilu. Vakuumisti IEVT so s svojim znanjem sodelovali v svetovno znanih institucijah kot npr.: SAES Geters, Heimann, Leybold Heraeus. Skupne rezultate so že takrat objavili v tuji znanstveni periodiki. Z raziskavami vakuumskih tankih plasti se je na IEVT intenzivno ukvarjal tudi prof. dr. Jože Gasperič, ki je problematiko kermetnih napršenih plasti obdelal v svojem magistrskem in nato še v doktorskem delu. Njegova temeljna spoznanja so pomembeno prispevala k razumevanju mehanizma rasti tankih napršenih plasti. Z izgradnjo eksperimentalnega ultravisoko vakuumskega sistema, opremljenega s spektrometrom Augerjevih elektronov na IEVT v sredini osemdesetih let pa je bila dana možnost raziskav fizikalno kemijskih procesov pri nastanku ultra tankih oksidnih plasti na površini tekočih kovin in zlitin "in situ". Tovrstne raziskave so bile izvedene prvič. Načrtovana in osvojena je bila nova eksperimentalna metoda, ki je omogočila študij začetnih stopenj rasti oksidnih plasti na tekočem indiju, ki smo ga tudi naparili in situ v spektrometru Augerjevih elektronov. Metoda je bila uporabljena tudi za študij ultra tankih segregiranih plasti Sb, Sn in Se na površini zlitin Fe-Si-C, mikrolegiranih z Sb, Sn ali Se. Študij ultra tankih plasti Sb, Sn, Se na dobro definiranih površinah Fe in V pa je predmet naših sedanjih raziskav, ki so vezane na nabavo novega AES/XPS instrumenta z visoko lateralno ločljivostjo. Prikazani so rezultati raziskav ultra tankih oksidnih plasti na tekočem indiju in zlitini InSn ter ultra tankih segregiranih Sb in Sn plasti na zlitini FeSiC.

Ključne besede: ultra tanke plasti, oksidacija, disociacija, In_2O_3, In_2O, Sb, Sn, površinska segregacija, AES, XPS

INTRODUCTION

Advanced technologies are strongly dependent on products of electronic industries such as optoelectronics, sensors, high density integrated components, etc. Thin films of thicknesses from ten to several hundreds of nanometers are very important in the production of these products. Ultrathin films-UTF whose thickness is up to few monoatomic layers are very decesive in the segregation, corrosion, recrystallization and catalytic processes. UTF are influenced by their interaction with the substrate and open a completly new perspective in the development of new advanced materials with desired physical and chemical properties.

Research, development and use of thin films started at the Institute for Electronics and Vacuum Techniques, IEVT, Ljubljana Slovenia after its foundation in early fifties. With the development of the miniature thin film potentiometers and thin films resistors of high stability at IEVT the first production of thin film electronic components in the country was established. The technology was successfully transferred to Slovenian factory in Cormons-Italy where the Slovenian minority is living.

Prof. Jože Gasperič was one of the leading scientists investigating the sputtered cermet thin films in his BS and Ph.D. works. His findings are basic for understanding the mechanism of growth of thin sputtered cermet films.

In the middle eighties the "high tech" research and development of the second and third generation image intensifier tubes was started at IEVT. An experimental ultra high vacuum, UHV, system equipped with Auger spectrometer, was built and the author was the first to investigate in situ the physical and chemical processes of ultra thin oxide film growth on the surface of liquid indium and indium alloys.

The experimental method based on Auger Electron Spectroscopy for the in situ investigation of the initial phase of ultra thin oxide film growth on liquid indium, was developed at the IEVT institute. The simplified experimental method was used for the investigation of segregated Sb, Sn or Se UTF on the surface of FeSiC alloy, microalloyed with Sb, Sn or Se at the Institute of Metals and Technology Ljubljana, where the first studies of P segregation started already in 1962.

The investigation of Sn, Sb or Se UTF on well defined Fe surfaces is being the topic of our present research work which is close connected with the purchase of new AES/XPS device with the very high spatial resolution.

The results of investigations of ultra thin oxide films on liquid In and InSn alloy as well as Sb, Sn and Se ultra thin film growth on the surface of FeSiC alloy are presented.

1 AES INVESTIGATION OF INITIAL PHASE OF LIQUID In AND InSn ALLOY OXIDATION AND DISSOCIATION OF In_2O_3

1.1 Fluxless vacuum soldering

In the production of the third generation image intensifier tubes the fluxless vacuum soldering is the most important process for hermetic encapsulation. Extremely clean surfaces are indispensable for obtaining good wetting of liquid solder. In the first model experiments we found that the leakage of fluxless vacuum soldered seals may often be caused by thin oxide film, covering the liquid solder. The solder is low melting InBi or InSn alloy. For the basic investigation we used pure indium as a solder and we realized that only in situ surface characterization may give direct insight into these complex surface phenomena.

For this purpose a very sensitive experimental method based on AES was developed at IEVT Ljubljana. The initial phase of surface oxidation on high purity in situ deposited indium and the mechanism of cleaning process of oxidised indium surface In_2O_3 was the main goal of the investigation.

1.2 Experimental method for the investigation of surface phenomena at fluxless vacuum soldering

The experiments were performed in an adapted Scanning Auger Electron Microprobe, additionally equipped with addapted sample holder, heater and thermocouple, evaporation source for in situ deposition of high purity indium, quartz microbalance for determination of In thin film thickness, quadrupole mass spectrometer-QMS for residual gas analysis and precise metal valve for oxygen introduction. Especially designed connections enabled the movement of the sample, **figure 1**.

The sample high purity indium thin film was deposited in situ on a pure molybdenum substrate. The oxide In_2O_3 film was obtained by exposure of the indium surface to pure oxygen at constant pressure $5x10^{-5}$ mbar with oxygen time exposure up to 100 minutes in temperature range from 25 to 250°C.

The resistive heater for investigating In/In_2O_3 film was a Mo strip which could be heated up to 1000°C. A thermocouple Fe-CuNi was welded on the rear side of the Mo strip. The indium source for in situ deposition was prepared from indium metal of 6N purity.

1.3 AES studies of the initial phase of liquid indium oxidation

The surface oxidation of indium in bulk and thin film occurs as (1):

$$4\ In\ (l) + 3\ O_2\ (g) \leftrightarrow 2\ In_2O_3\ (c) \qquad (1)$$

where (c), (l) and (g) mean crystalline, liquid and gas state, respectively. The solubility of oxygen in pure liquid indium is extremely low, $1x10^{-6}$ atomic percent at 550°C and it is negligible in the temperature range of our investigation from 25 to 250°C. The diffusivity of

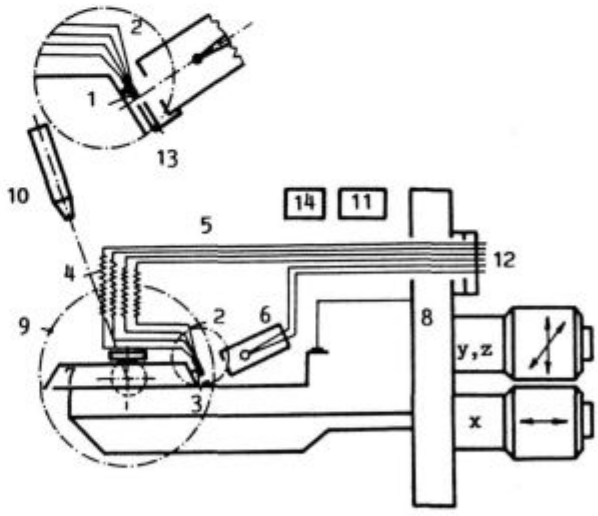

Figure 1: AES spectrometer adapted for liquid indium surface investigations: 1 - sample, 2 - Thermocouple, 3 - sample holder, 4 - flexible connections, 5 - rigid connections, 6 - In source for in situ evaporation, 8 - flange, 9 - CMA, 10 - ion gun, 11 - QMS, 12 - lead through, 13 - quartz microbalance, 14 - metal valve for oxygen introduction

Slika 1: Spektrometer Augerjevih elektronov prirejen za raziskave procesov na tekočem indiju: 1 - vzorec, 2 - termočlen, 3 - nosilec vzorca, 4 - gibljivi priključki, 5 fiksni priključki, 6 - In izvir za "in situ" naparevanje, 8 - prirobnica, 9 - CMA, 10 - ionska puška, 11 - QMS, 12 - prevodnice, 13 - kremenova mikrotehtnica, 14 - vpustni ventil za kisik

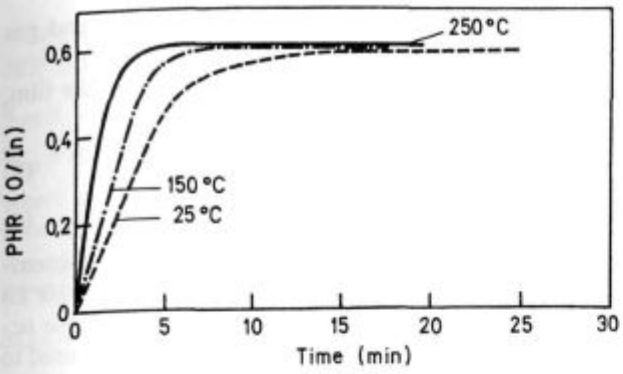

Figure 2: Surface oxidation rate of crystalline and liquid indium at temperatures 25, 150 in 250°C at a constant oxygen pressure of $5x10^{-5}$ mbar

Slika 2: površinska oksidacija trdnega in tekočega indija pri temperaturah 25, 150 in 250 °C in konstantnem tlaku kisika $5x10^{-5}$ mbar.

oxygen in liquid indium is very low, $3.7x10^{-7}$ cm^2 s^{-1} at 550°C.

It was concluded from these facts that the process of pure liquid indium oxidation occurs at the surface.

The kinetics of thin oxide film growth on crystalline and liquid indium was investigated by AES, following the peak height ratio-PHR of amplitudes between O(KLL) and In ($M_5N_{45}N_{45}$) Auger transition at kinetic electron energies of 512 eV and 402 eV (for In^0) and 405 eV (for In^{3+}) respectively. For a defined geometrical sample position in the AES spectrometer, the kinetics of the thin oxide film growth was followed up to the film thickness of 3.5 nm, which corresponds to an effective electron depth escape λ_{ef} for In_2O_3.

Surface indium oxidation was investigated at the temperatures of 25, 150, 250 in 550°C, **figure 2**.

Thin oxide film thickness of 3.5 nm on pure indium were obtained at conditions listed in **Table 1**.

Table 1: In_2O_3 films, 3.5 nm thick obtained at different temperatures and different oxygen exposures

Temperature (°C)	Oxygen exposure (L)
25	$6x10^4$
250	$3x10^4$
550	$1.5x10^4$

At higher temperatures T > 360°C, a volatile oxide was formed by the reaction:

$$In_2O_3\ (c) + 4\ In\ (l) \leftrightarrow 3\ In_2O\ (g) \qquad (2)$$

The reaction between the In_2O_3 thin film and the underlying liquid indium, corresponding to equation (2) was studied at the temperature of 360, 400, 450 and 550°C in vacuum of $1x10^{-9}$ mbar. The results are shown in **figure 3**.

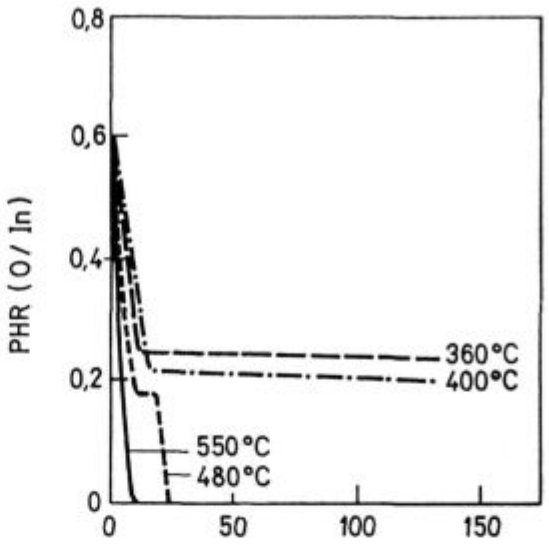

Figure 3: Isothermal dissociation of In_2O_3 ultra thin solid film on liquid indium at the temperatures 360, 400, 450 in 550°C in a vacuum below $1x10^{-9}$ mbar

Slika 3: Izotermna disociacija ultra tanke plasti In_2O_3 na tekočem indiju pri temperaturah 360, 400, 450 in 550 °C in vakuumu pri tlaku < $1x10^{-9}$ mbar.

1.4 Investigation of In_2O_3 dissociation in uhv by AES

At temperature T > 360°C the evaporation of volatile In_2O corresponding to equation (2) proceeded with perceivable velocity. At 550°C the process was so fast that AES studies of In_2O_3 to In were not possible.

The use of indium as a solder for vacuum fluxless soldering depends upon the fact that the thin In_2O_3 film spontaneously disappeared - dissociated at T > 360°C by In_2O evaporation following the equation (2) In_2O_3 (c) + 4 In (l) ↔ 3 In_2O (g).

1.5 AES investigation of initial phases oxidation of InSn liquid solder

In the second part of our investigation the knowledge of the initial phase of surface oxidation on pure liquid In to InSn solder (20 at.% In, 80 at% Sn) was applied. The samples high purity InSn film, 2.5 μm thick were prepared in Balzers Sputron plasma beam apparatus, **figure 4**.

On the oxidised InSn surface a difference between AES spectra of pure metal In (402, 408 eV) and In_2O_3 (399, 405 eV) was found. For tin (428, 435 eV) the characteristic chemical shift was not determined and only changes in the shape and intensity of Auger spectra were recognized.

Figure 5 shows the AES spectra of the liquid InSn alloy exposed to pure oxygen $1.5x10^4$ L, covered by thin oxide film, approximately 3.5 nm thick **(figure 6)**, corresponding to an effective electron depth escape λ_{ef} for In_2O_3.

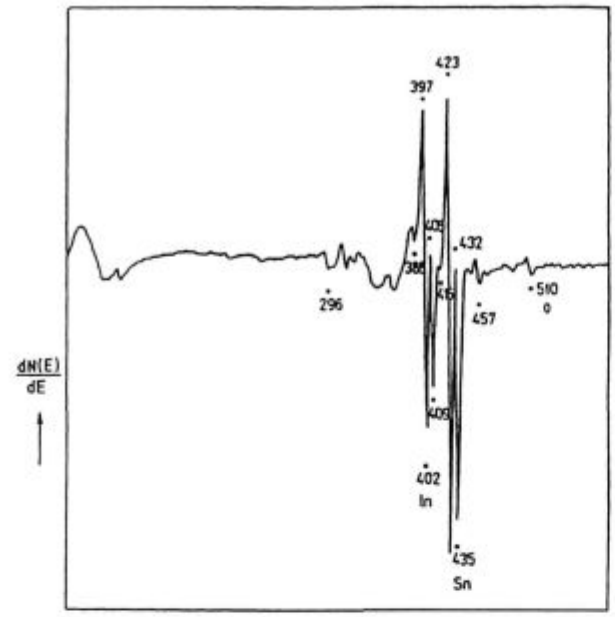

Figure 4: AES spectrum of InSn solder (20 at.% In and 80 at% Sn) after ion etching approximately 3 nm under surface

Slika 4: AES spekter InSn spajke(20 at.% In and 80 at% Sn) po ionskem jedkanju približno 3nm pod površino

The samples were oxidised in situ in Auger Spectrometer by exposure of a clean surface of liquid InSn alloy to pure oxygen (10^4 - 10^6 L) at 250°C.

The results indicate that all oxide films on the surface of liquid InSn solder were enriched in indium in varying amounts, depending on oxygen pressure, time exposure etc.

In the first part of the investigation it was found that the surface oxidation of In, in bulk or in the form of a thin film can be formulated by equation (1):

$$4\ In\ (l) + 3\ O_2\ (g) \leftrightarrow 2\ In_2O_3\ (c) \qquad (1)$$

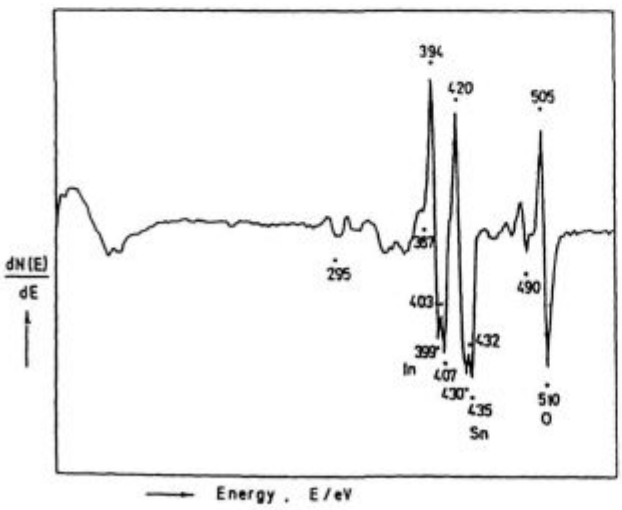

Figure 5: AES spectrum of 3.5 nm thick oxide UTF on the surface of liquid InSn alloy

Slika 5: AES spekter 3.5 nm debele oksidne plasti na površini tekoče spajke InSn.

where (c), (l) and (g) mean crystalline, liquid and gas state, respectively.

The surface oxidation of Sn, in bulk or in thin film, occurs by the reactions:

$$2\ Sn\ (l) + O_2\ (g) \leftrightarrow 2\ SnO\ (c) \qquad (3)$$

$$Sn\ (l) + O_2\ (g) \leftrightarrow SnO_2\ (c) \qquad (4)$$

AES chemical shifts of SnO and SnO_2 are approximately the same. On tin exposed to oxygen (10^4 - 10^6 L) both oxides SnO and SnO_2 were found. As the same occurs for SnO and SnO_2, chemical shift can not be used to identify the oxidized state of the tin film. It was proposed that a mixture of oxides SnO, SnO_2 and In_2O_3 was formed on InSn alloy at the exposure to oxygen (10^4 - 10^6 L). The mixture of oxides appeared to be thermodynamically unstable near the alloy-oxide interface; SnO and SnO_2 oxides were reduced to Sn with the tendence to the formation of additional In_2O_3

$$3SnO_{(oxide,c)} + 2In_{(alloy,l)} \leftrightarrow In_2O_{3(oxide,c)} + 3Sn_{(alloy,l)} \qquad (5)$$

$$3SnO_{2(oxide,c)} + 4In_{(alloy,l)} \leftrightarrow 2In_2O_{3(oxide,c)} + 3Sn_{(alloy,l)} \qquad (6)$$

Free energy ΔG^o of reactions (5) and (6) are obtained by using the data for free energy of formation SnO, SnO_2 and In_2O_3

$$\Delta G^o(SnO) = \\ = -69670 + 3.06\ T\log T - 1.5\times10^{-3}T^2 - 0. + 18.39T \qquad (7)$$

$$\Delta G^o(SnO_2) = -143080 - 7.37\ T\log T - \\ - 0.7\times10^{-3}T2 + 2.38\times10^5T^{-1} + 76.53T \qquad (8)$$

$$\Delta G^o(In_2O_3) = -220970 + 24.22T\log T - \\ 3\times10^{-3}T^2 - 0.3\times10^5T^{-1} + 41.36T \qquad (9)$$

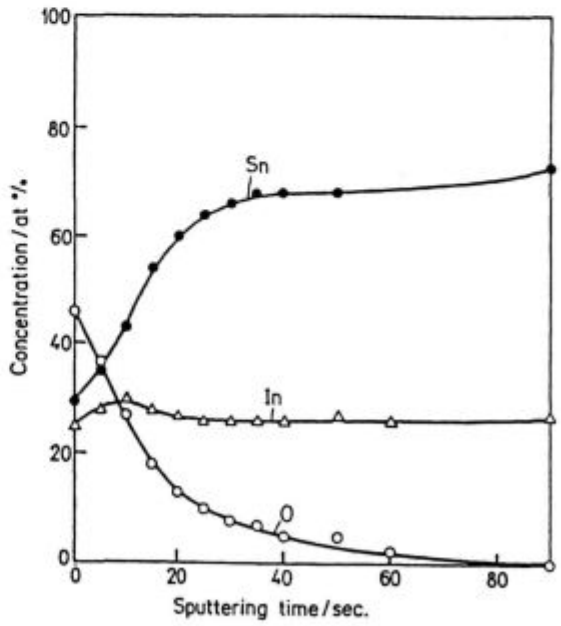

Figure 6: AES depth profile of oxide UTF on surface of liquid InSn solder. Oxide UTF was made in situ

Slika 6: AES profilni diagram ultra tanke oksidne plasti na tekoči spajki InSn; oksidna plast je bila narejena *in situ*

At the temperature 250°C ΔG° (5) = -525 kJmol^{-1} and ΔG° (6) = -285 kJmol^{-1} and the equilibrium constants:

$$K_{(5)} = (a_{Sn}^3 \times a_{In2O3})/(a_{SnO3} \times a_{In2}) = 2.2\times10^{52} \quad (10)$$

$$K_{(6)} = (a_{Sn}^3 \times a_{In2O3}^2)/(a_{SnO}^3 \times a_{In}^4) = 2.8\times10^{28} \quad (11)$$

where a_i s are the activities of the reactants and products. The mixed oxide thin film formed during oxidation would be a mixture of pure In_2O_3, SnO and SnO_2. The driving force for reactions (5) and (6) is therefore

$$\Delta G_{(5)} = \Delta G^{\circ} + RT \ln[(1 - N_{In})^3/N^2_{In}] \quad (12)$$

$$\Delta G_{(6)} = \Delta G^{\circ} + RT \ln[(1 - N_{In})^3/N^4_{In}] \quad (13)$$

N_{In} is the indium concentration in the SnIn alloy. At 250°C ΔG for N_{In} 10^{-6} (1ppm) is -108 kJmol^{-1} for reaction (5) and -351 kJmol^{-1} for reaction (6).

In other words, SnO and SnO_2 are thermodynamically unstable are in the mixed oxide even when in contact with extremely dilute In in Sn. The only stable oxide formed at InSn alloy should be In_2O_3 at 250°C. Since all oxidation processes are of the nonequilibrium type, the amounts of SnO and SnO_2 and the overall SnO, SnO_2/In_2O_3 ratio depend on O_2 pressure, temperature, diffusion coefficient, solubilities and other factors. Consequently the mixed oxides SnO and SnO_2 in the oxide-alloy interface tend to be converted into Sn and In_2O_3.

1.6 AES investigation of In_2O_3 dissociation on the surface of liquid InSn solder in UHV

The last part of fluxless vacuum soldering in UHV investigation dealt with the "cleaning process" by dissociation of thin In_2O_3 film from the surface of the liquid InSn solder. The reaction between the thin In_2O_3 film and the underlying liquid InSn solder correspond to equation

$$4\ In\ (l) + 3\ O_2\ (g) \leftrightarrow 2\ In_2O_3\ (c) \quad (1)$$

was investigated at 550°C and the results are shown in **figure 7**. It was found that at T>250°C in UHV the thin In_2O_3 film formed on the surface of liquid InSn alloy spontaneously disappeared by In_2O_3 dissociation according to equation (1). The oxides SnO and SnO_2 or In_2O_3 are unstable in very thin oxide films on the surface of a liquid InSn solder at T>250°C.

For fluxless vacuum vacuum soldering with liquid indium, previously cleaned at T > 360°C, recontamination is negligible in UHV in the temperature range:

Tm < T < 360°C

At fluxless vacuum soldering with liquid InSn solder, previously cleaned at T > 360°C, recontamination is negligible in UHV in the temperature range Tm < T < 360°C.

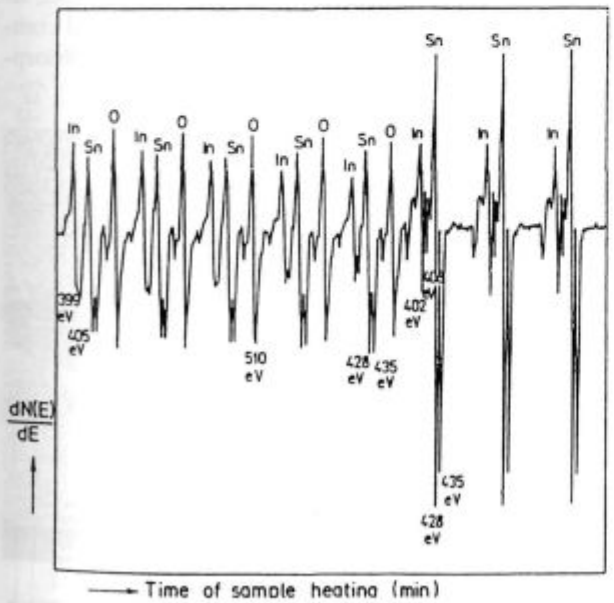

Figure 7: Changes in AES peaks of In, Sn and O between heating of oxidized InSn solder at constant temperature of 450°C

Slika 7: Spremembe AES vrhov značilnih za In, Sn in O med segrevanjem oksidirane spajke InSn pri konstantni temperaturi 450°C

2 CHARACTERIZATION OF SEGREGATED Sb AND Sn UTF BY AES

2.1 Introduction

Physical properties of metals and alloys depend on the composition and on the surface and interface structure of the material. These properties are affected by segregation processes of alloying elements and impurity elements during their manufacturing and use. Some of these elements which segregates on free surfaces (surfaces, grain boundaries, interfaces) and ultra thin segregated films specifically affect adsorption, corrosion, adhesion, surface diffusion, recrystallization, catalytic activity, friction and wear[7-8].

The atomic composition of grain boundaries is also very important because it affects physical properties as well as corrosion behaviour of metals and alloys. For materials applied at high temperatures, the composition of interfaces may be drastically changed by segregation, by enrichment of dissolved surface active atoms diffusing on the surface or grain boundaries and can cause metal embrittlement.

The aim of the investigation was to examine the nature of segregation of antimony and tin and its effect on recrystallization process, grain growth and texture development of a cold rolled and annealed silicon non oriented electrical sheet to be used in generation of electrical energy.

It has been experimentally confirmed that a small addition of antimony, tin and selenium into the melt of silicon iron by microalloying affect the magnetic properties of electrical sheets by enrichment on free surfaces, i.e. surfaces and grain boundaries[9-13,15-19].

Such enrichment affects grain growth, producing an increase in the number of ferrite grains with soft magnetic lattice orientation which grow on the account of grains with other crystallographic orientations, and in

this way improves the magnetic properties. Our investigations show a strong correlation between antimony and tin surface segregation and the orientation of surface grains[17-19].

The kinetics of surface segregation is determined by bulk diffusion of the segregate to the respective interface. Surface segregation kinetics was measured on non oriented silicon steel sheet in situ by Auger Electron Spectroscopy-AES, by annealing and simultaneous analysis of the sputter cleaned sample at higher temperature in UHV.

Non oriented silicon steel is a polycrystalline multicomponent alloy of Fe, Si, Al, C, P and S. The addition of approximately 0.05 to 0.1% of single elements i.e. antimony or tin starts a competition for free surface sites[7,25].

The grain boundary segregation of Sb and Sn was studied initially on polycrystalline non oriented silicon steel. The alloys were annealed in the temperature range between 450 and 650°C to establish the equilibrium grain boundary segregation on samples quenched and mounted into UHV system, fractured in situ after cooling and analysed by AES.

The main point of the research work was the determination of the physical nature of the surface segregation and its relationship to the internal grain boundary segregation grains at the sheet surface. The investigation also included the determination and evolution of the texture of grains at the sheet surface. Emphasis was placed on the understanding how texture affects the electrical energy losses, as well as magnetic properties.

2.2 Surface segregation of antimony and tin

Most elements dissolved in iron tend to enrich at elevated temperatures at surfaces, grain boundaries and interfaces and distribution equilibrium $A_{dissolved} \leftrightarrow A_{segregated}$ are established at sufficiently high temperature[7,25,26,34].

2.2.1 Antimony

Antimony surface segregation was studied using AES method on a 2.0% Si steel, alloyed with different mass contents of Sb (0.05 and 0.1%). The dependence of surface segregation on grain orientation and on the presence of other solute atoms of S, P, C, Al and Si was investigated in situ under UHV conditions by AES in the temperature range from 450 to 900°C.

The antimony enrichment at the surface was estimated by following the peak height ratio - PHR of amplitudes between the dominant $Sb(M_5N_{4,5}N_{4,5})$ and $Fe(L M_{2,3}V)$ Auger transitions at kinetic energies of 454 and 651 eV, respectively.

The mole fraction of Sb 0.05% and 0.1% in investigated steels, is clearly in the range of solubility in α-Fe at all temperatures investigated but below the detection limit of AES method. The enrichment of Sb, caused by equilibrium segregation at the surface, can only be measured at or after annealing at elevated temperatures by AES method.

AES measurements showed a different quantity of segregated antimony on different grains (**figure 8**). All samples were metalographically polished, the orientation of single grains was determined by the etch pitting method. The temperature dependence of antimony surface segregation a) on grain with (001) and b) (111) orientation is shown on **figure 9**.

The surface of investigated steel alloyed with 0.1% Sb was clean sputtered with Ar^+ ions and in situ annealed in the analyzing chamber of the Auger spectrometer. The temperature was increased every 20 minutes for 50°C. The antimony segregation rate was perceived at temperature T > 650°C and it increased with the increasing temperature, while at T > 850°C the antimony segregation rate declined. If the influence of a possible channelling effect is neglected, it is possible to estimate the Sb surface concentration by comparison with the results on Sb surface segregation on single crystal surfaces of Fe - 4% Sb of defined orientation. For the same primary energy of exciting electrons, the saturation PHR were measured for single crystal surfaces of (100), (110) and (111) orientation. For the (100) oriented surface, the saturation coverage is half of a monolayer corresponding to LEED c(2x2) overlay pattern. For other surface orientations, no well defined ordered structure of surface coverage was observed. The PHR was of the same order; for (111) oriented grain 0.6, and for (100) oriented grain 0.4. In the investigated steels other solute elements such as C, S and P are present. Two or more elements can simultaneously segregate to the surface. In such cases a competition for the sites available occurs[24-32]. The relative amount of segregating elements on the surface depends on their free energy of segregation and their concentration in the bulk[29-32,347-37]. Also the kinetics of antimony surface segregation was measured (**figure 10**).

There are two possible explanations for this effect, simultaneous antimony and sulphur segregation and competition for sites available on the surface, and/or desorption from the segregated layer.

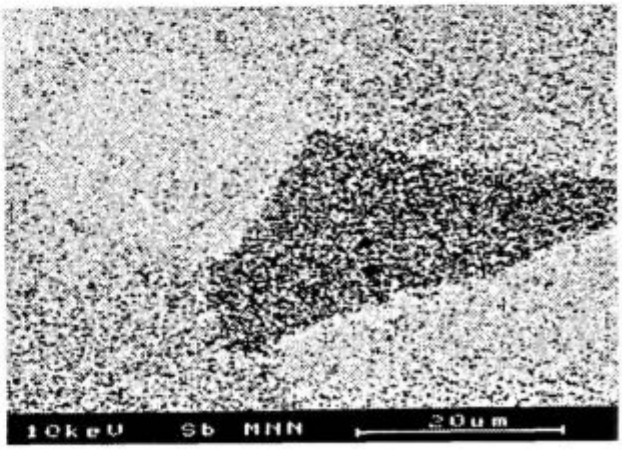

Figure 8: SAM image of the surface of steel with 0.05% Sb. A different quantity of segregated antimony was measured on grains with different orientation in the plane of the sheet

Slika 8: SAM posnetek površine jekla legiranega z 0.05%Sb. Površinska segregacija Sb je odvisna od kristalografske orientacije zrn.

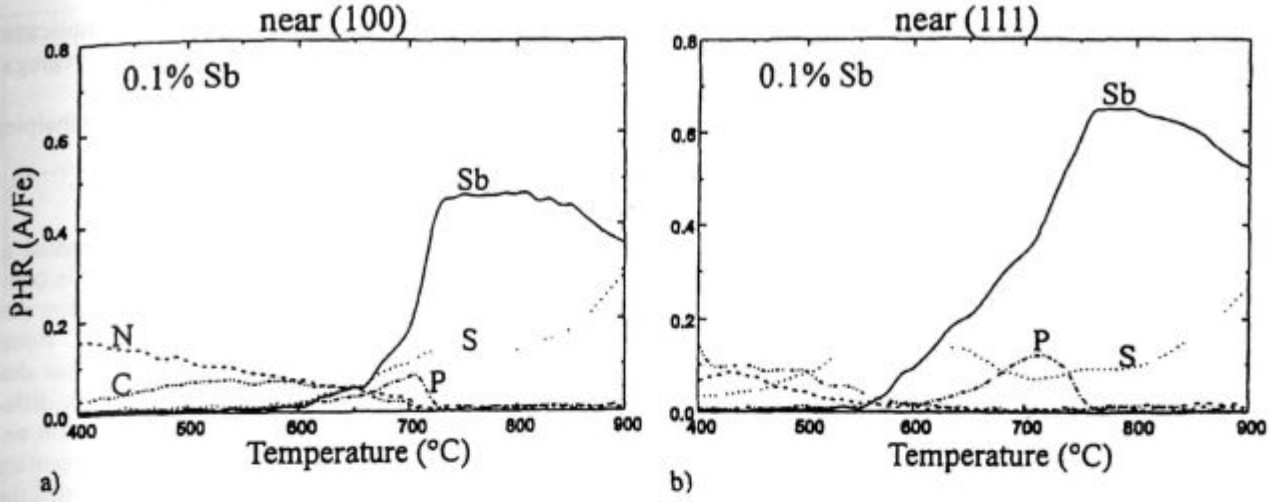

Figure 9: Temperature dependence of surface segregation on steel with 0.1% Sb on a) (100) and b) (111) oriented grain
Slika 9: Temperaturna odvisnost površinske segregacije na jeklu z 0.1%Sb a) na zrnu (100), b) na zrnu (111)

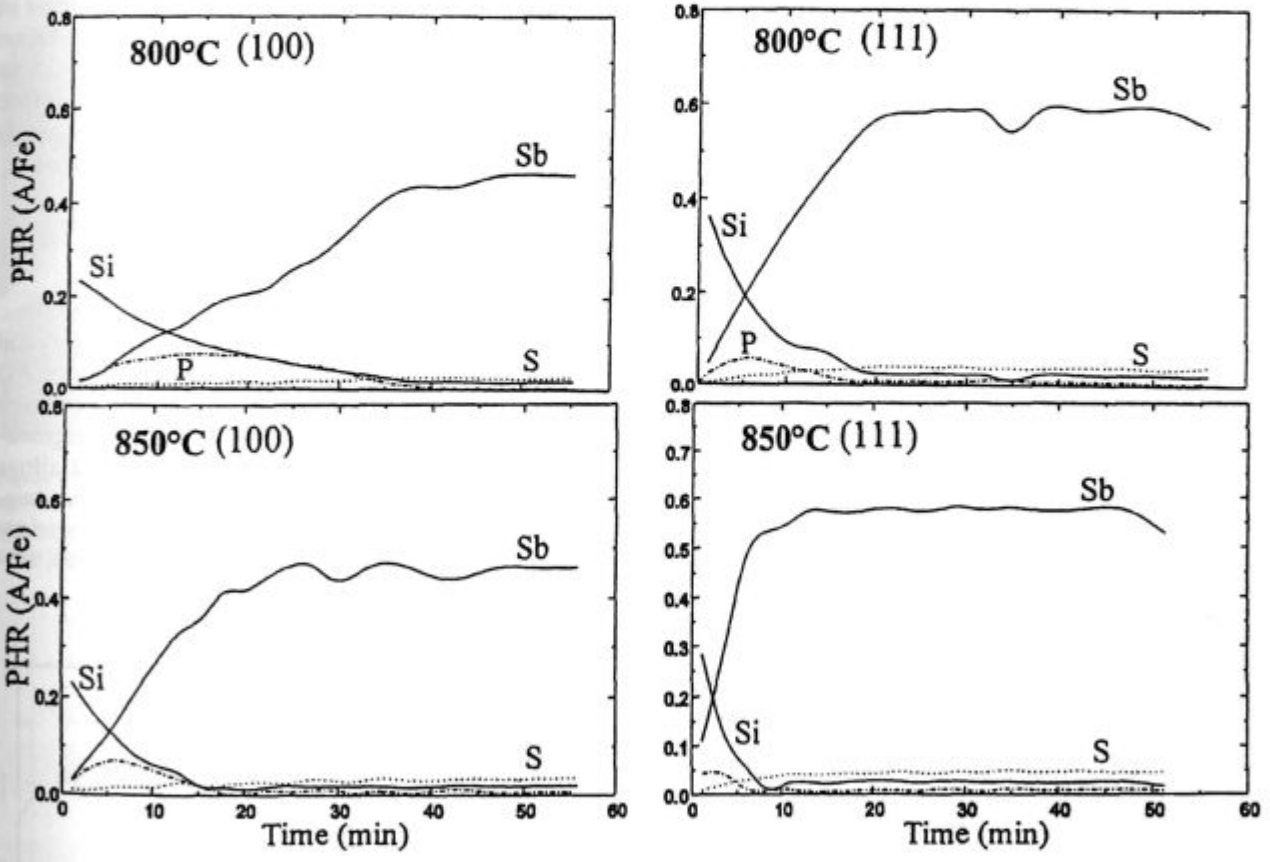

Figure 10: Sb surface segregation on steel with 0.1% Sb on a) (100) and b) (111) oriented grain at 800 and 850°C
Slika 10: Površinska segregacija Sb na jeklu z 0.1% Sb a) (100) zrno in b) (111) zrno pri 800 in 850 °C

The competitive surface segregation of antimony and sulphur is described by the following equations[25]:

$$\frac{\Theta_{Sb}}{1-\Theta_{Sb}-\Theta_S} = x_{Sb}\exp(-\Delta G_{Sb}/RT) \quad (1)$$

$$\frac{\Theta_{Sb}}{1-\Theta_S-\Theta_{Sb}} = x_{Sb}\exp(-\Delta G_S/RT) \quad (2)$$

where Θ_{Sb} and Θ_S are saturation coverage, χ_{Sb} and χ_S are mole fractions and ΔG_{Sb} and ΔG_S are free energies

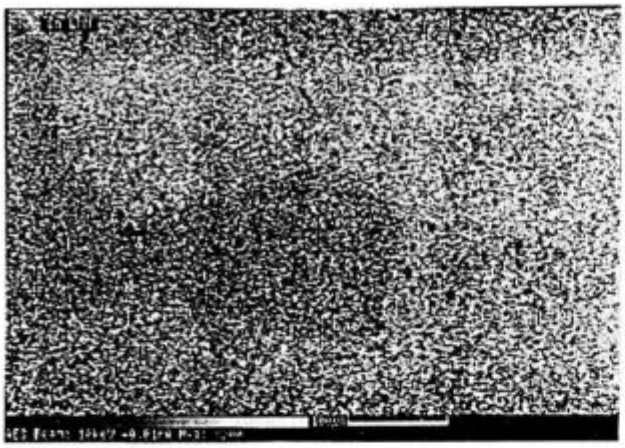

Figure 11: SAM image of the surface of steel with 0.1% Sn. A different quantity of segregated tin was measured on grains with different orientation in the sheet plane
Slika 11: SAM posnetk površine jekla z 0.1% Sn. Površinska segregacija Sn je odvisna od kristalografske orientacije zrn v ravnini pločevine.

of Sb and S surface segregation, respectively, R is the specific gas constant, and T absolute temperature.

Antimony desorption from segregated layer was established using Thermal Desorption Spectrometry -TDS at T > 750°C.

2.2.2 Tin

A scanning Auger image - SAM of non-oriented electrical steel annealed 10 minutes at 800°C was taken. The orientation of individual grains was determined by the etch pit method. **Figure 11** shows SEM and SAM images of the surface of the investigated steel. A different surface tin segregation rate on different grains was measured. Different grain orientation provided different sites for segregated tin atoms.

Figure 12 shows the temperature dependence of surface segregation of alloying and tramp elements of non-oriented electrical steel alloyed with 0.05% Sn on grain orientations (001) and (111) respectively. Electrical steel is a multicomponent system with a very complicated temperature dependence behaviour of surface segregation on binary alloys.

The relations of the surface segregation enthalpies and volume diffusivitiy are as follows:

$\Delta H^0_{Si} < \Delta H^0_C < \Delta H^0_P$ and $D^C_V >> D^{Si}_V > D^P_V$

At lower temperature, about 300°C, C segregated to the surface due to very high diffusion coefficient in comparison to Si and P, although the bulk concentration was very low, only 15 ppm. At higher temperature, C atoms were displaced by Si atoms and P while S atoms displaced silicon at higher temperatures. Their bulk diffusion coefficient is rather low, but their segregation enthalpy is very high, therefore tin started segregating significantly above 600°C. Kinetics study confirmed the orientation dependence of tin surface segregation and of the thickness of the segregated layer.

It was ascertained[17] that on grains with (100) and (111) orientation in the sheet plane, the segregation of tin was beyond one monolayer, due to the strong decrease of surface energy. On a surface with a (111) orientation FeSn intermetallic compound of one unit cell thickness was found. Our measurements showed that tin surface coverage dependence on tin bulk concentration and Θ value approached one for (100) and (111) orientations.

2.3 Grain boundary segregation

2.3.1 Antimony

Grain boundaries of FeSi steel alloyed with 0.05 and 0.1% Sb were also analyzed by AES after ageing for 200 and 500 hours at 550°C. The fracture facets were almost completely transgranular, only on some areas intergranular decohesion was noticed. In the investigated alloys there was no indication of antimony grain boundary segregation (**figure 13**). Only a negligible grain boundary segregation of other solute elements such as carbon, silicon and aluminium was established.

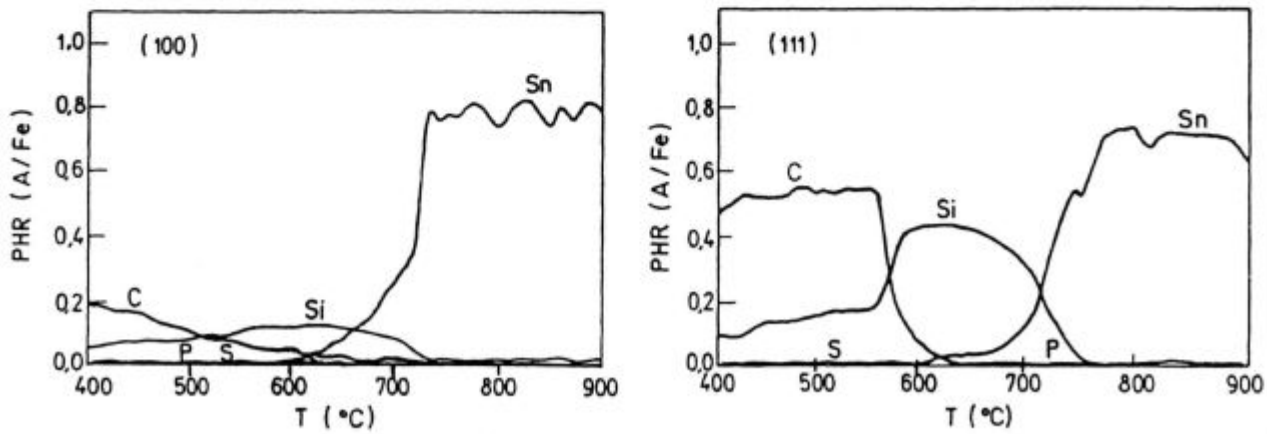

Figure 12: Temperature dependence of surface segregation on steel with 0.1% Sn on a) (100) and b) (111) oriented grains
Slika 12: Temperaturna odvisnost površinske segregacije na jeklu z 0.1%Sn a) (100) in b) (111) orientirana zrna.

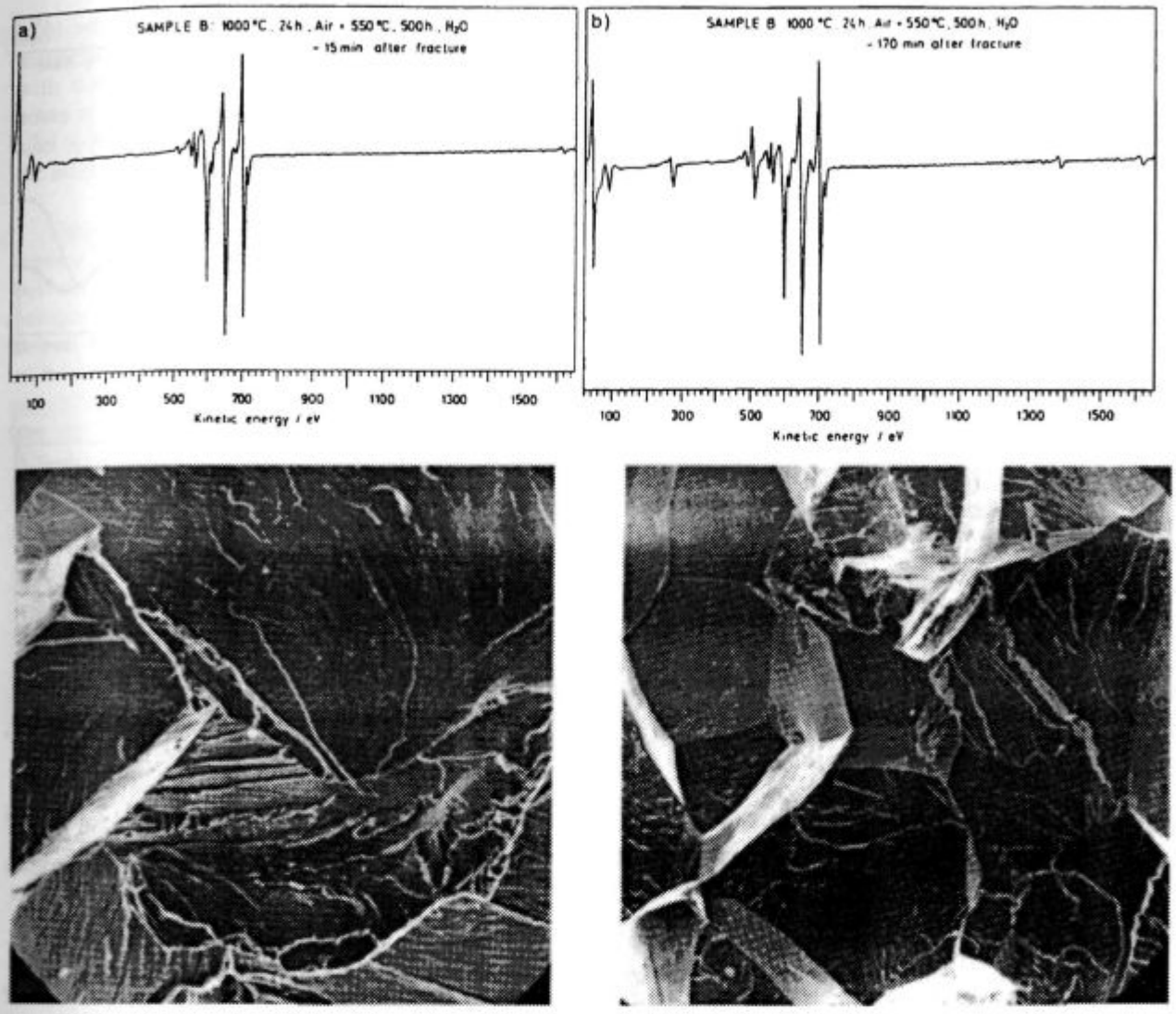

Figure 13: AES spectra taken on a) transgranular facets and SEM image of fractured sample and b) an intergranular facet of non oriented silicon steel with 0.1% Sb and SEM image of transgranular facet

Slika 13: AES spekter posnet na a) transkristalni ploskvi in SEM posnetek prelomljenega vzorca in b) interkristalni prelom silicijevega jekla za neorientirano pločevino z 0.1%Sb

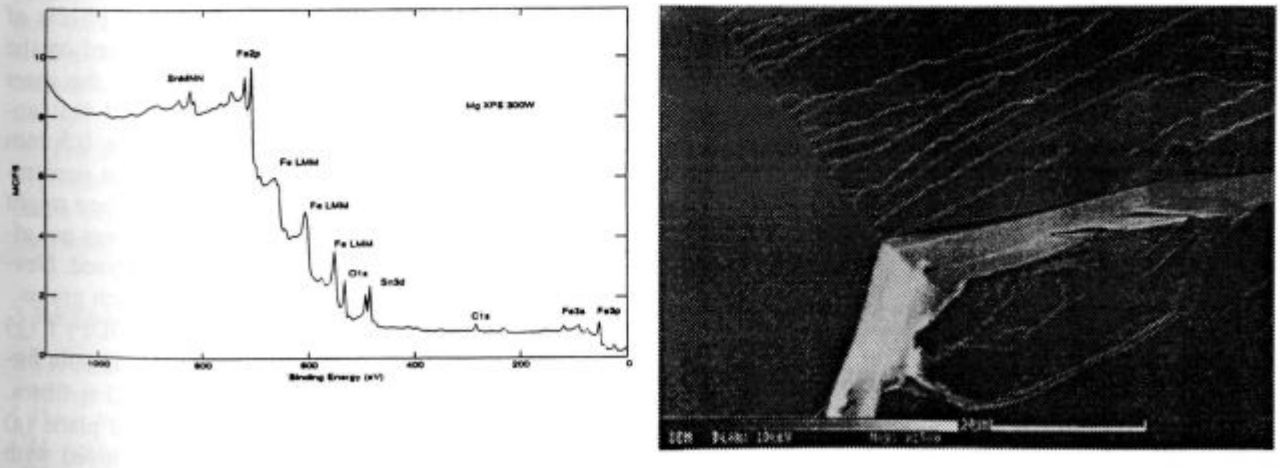

Figure 14: XPS spectra taken on intergranular facet and SEM image of fractured non oriented silicon steel with 0.1% Sn

Slika 14: XPS spekter posnet na interkristalni ploskvi in SEM posnetek prelomljenega vzorca silicijevega jekla za neorientirano elektro pločevino z 0.1%Sn

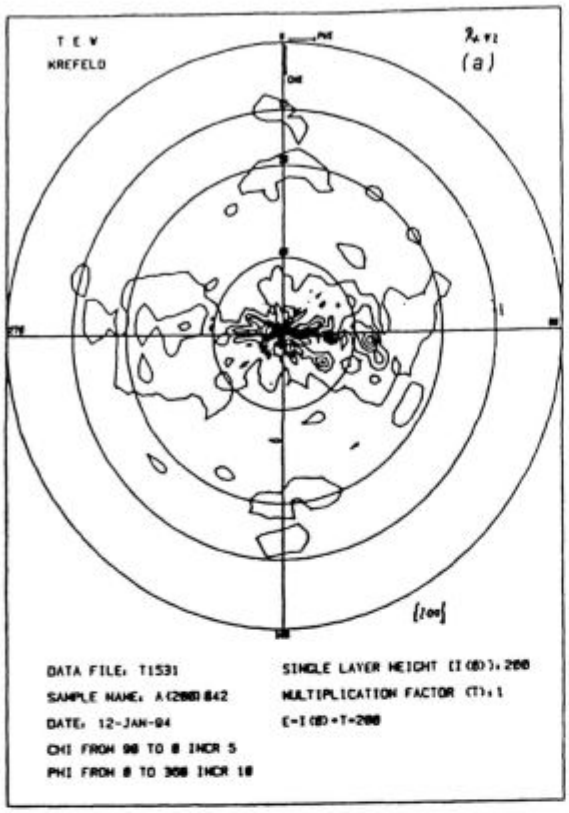

Figure 15: Pole figure of (200) grains obtained by X-ray difractometry shows the share of grains with (001)(100) texture in the steel sheet with 0.05% Sb

Slika 15: Polove figure zrn (200) narejene z rentgensko difraktometrijo prikazujejo delež zrn (001)(100) v teksturi elektro pločevine z 0.05% Sb.

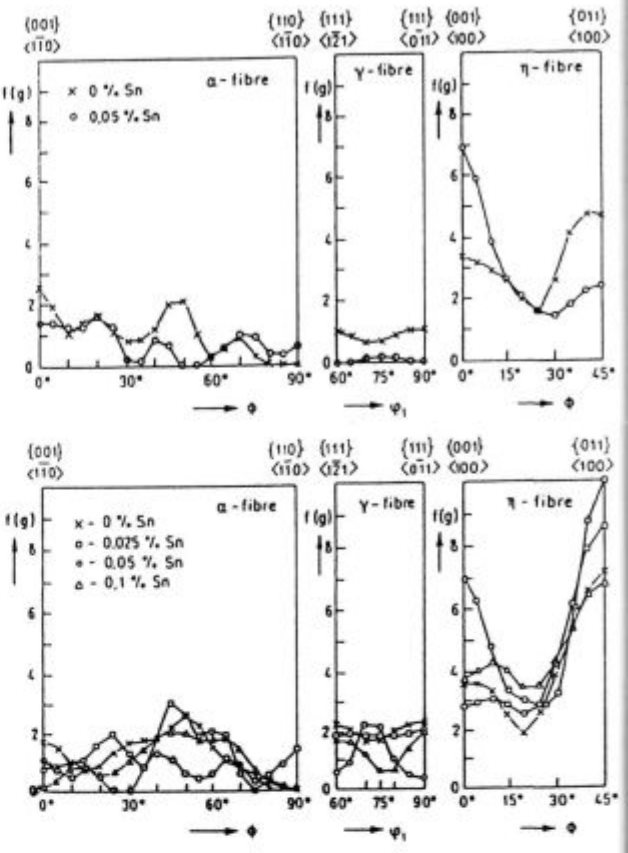

Figure 16: Texture fibres in the middle plane a) and b) on the surface of electrical steel with 0.05% Sn and without Sn

Slika 16: Tekstura vlaken v sredini vzorca a) in b) na površini elektro pločevine z 0.05% Sn in brez Sn.

2.3.2 Tin

The equilibrium segregation of tin was attained after annealing the specimen alloyed with 0.1% Sn for 200 hours at 550°C, **figure 14**.

Considering that tin is equally distributed on both fractured sides, a coverage of grain boundary surface of 0.05 ML was estimated. The scattering of results was rather large due to the strong dependence of tin segregation to grain boundary orientation. Steel alloyed with 0.05% Sn had much less intergranular facets. The evaluated equilibrium segregation was smaller than in steel alloyed with 0.1% Sn. Detailed AES analyses of free surfaces between inclusion (AlN, Al_2O_3) and matrix clearly indicated that a considerable tin segregation occurs also at their interfaces.

2.4 Texture determination

2.4.1 Antimony

The results support the hypothesis that the texture formation results from orientation dependent effects of antimony and tin on the surface energy. The texture of sheets from antimony and antimony free steels was determined by X-ray difractometry. The pole figure obtained (**figure 15**), shows that only a small share of grains with (001)(100) texture was found in the investigated 0.05% Sb steel.

2.4.2 Tin

The results support the hypothesis that the texture formation results from orientation dependent effects of tin on surface energy. The texture was measured on the surface and in internal plane after the half of the sheet thickness was removed. Taking into account that approximately six crystal grains constitute the 0.5 mm thick cross-section steel sheet and the fact that penetration depths of X-rays was less than 0.01 mm one might conclude that also some grains whose growth was not affected by the surface tin segregation were analysed. Nevertheless, there were not more than 10% of such grains.

The orientation distribution functions (ODF) f (g) were calculated from the (200), (110) and (211) pole figures. The textures were presented as α, γ and η fibres. **Figure 16** shows texture fibres in the internal plane (a) and on the surface (b) of electrical steels alloyed with and without tin. The volume fraction of grains with the (100) planes measured on the surface and in the middle plane increased by the order of two when compared the

steel without tin and the steel with 0.05% tin. Softer magnetic orientations were found on the surface. Steel with 0.05% Sn, which had previously been aged 25 hours at 550°C, showed an increase of (100) planes parallel to the rolling direction by three times, compared to the steel without tin.[36]

During annealing antimony and tin segregated at steel surface at temperatures T > 650°C. A strong correlation between the antimony or tin surface segregation and the orientation of the grains at the sheet surface was established. The maximum equilibrium Sb surface segregation of 0.6 monolayer was measured after annealing at 750°C on grains with the (111) crystallographic orientation in the sheet plane. The maximum equilibrium Sn segregation on the surface was reached also at 750°C and approached in the majority of orientations one monolayer.

Grain boundary segregation of antimony and other solute elements, such as C, S, P, Al and Si were negligible in non oriented silicon steel with 0.05 and 0.1% Sb.

Tin surface segregation was much higher than grain boundary segregation. At equilibrium grain boundary segregation only 7 and 3% of tin atoms were found on a grain boundary for steel alloyed with 0.1 and 0.05% Sn, respectively.

Antimony as well as tin surface segregation decreased the surface energy of grains with (100) surface orientation in the sheet plane, and these grains grow on account of grains with other surface crystallographic orientations, such as (110) and (111). Only a certain level of surface segregation promoted selective grain growth. By excessive surface coverage of segregated atoms, the surface energy of all orientations is not affected selectively and no preferential grain growth is obtained.

Textures represented as sections through three-dimensional orientation distribution space in fixed directions showed that the volume fraction of magnetically soft grains increased for three times in tin steel sheets when compared to steel without tin. Better textures were obtained near the surface than in the middle plane of 0.5 mm thick steel sheet. The best results were obtained for steel alloyed with 0.05% Sn. It is concluded that only a certain level of segregation promoted the desired selective grain growth.

The results of the present investigation support the hypothesis that the texture formation results from orientation dependent effects of antimony and tin on the surface energy.

3 REFERENCES

[1] I. P. Csorba, *Image Tubes*, Howard W. Sams, Indianapolis 1985

[2] M. Jenko, *Surface phenomena at Fluxless vacuum soldering* Ph.D Thesis, University of Ljubljana, Ljubljana 1988

[3] M. Jenko, B. Erjavec, B. Praček, *Vacuum*, 40 (1990) 77

[4] M. Jenko, S. Jerič, B. Praček, B. Erjavec, *Vuoto*, Vol. XX. N2 (1990) 350

[5] D. Brigs, M. P. Seah Eds, *Practical Surface Analysis, Vol. 1 Auger and X-ray Photelectron Spectroscopy* 2nd Edition, John Wiley&Sons Chichester 1994

[6] R. C. Weast, M. J. Astle, Eds, CRC Handbook of Chemistry and Physics, 76th Edition, Chemical Rubber, Palm beach 1995/96

[7] O. Kubaschewski, C. B. Alcock, P. J. Spencer, *Materials Thermochemistry*, 6th Edition, Pergamon, Oxford 1993

[8] H. J. Grabke, *Iron and Steels, ISIJ Int.*, 35 (1995) 2, 95-113

[9] G. Lyudkovski, P. K. Rastogi, *Metall. Trans. A.*, 15A (1984) 257

[10] H. Shimanaka, T. Irie, K. Matsumura and K. Nakamura, *J. Magn. Magn. Mat.*, 19 (1980) 63

[11] P. Marko, A. Šolyom, V. Frič, *J. Magn. Magn. Mat.*, 41 (1984)

[12] S. Nakashima, K. Takashima, J. Harase and K. Kuroki, *J. Japan Inst. Metals*, 55, (1991) 12, 1392-1399

[13] F. Vodopivec, F. Marinšek, D. Gnidovec, B. Praček, M. Jenko, *J. Magn. Magn. Mat.*, 97 (1991) 281

[14] F. Kovač Niznik, *Metallography 95*, Proceedings, Slovakia, April 1995, Paper 14, 84-87

[15] M. Jenko, F. Vodopivec, B. Praček, *App. Surf. Sci.*, 70/71 (1993) 118

[16] M. Jenko, F. Vodopivec, B. Praček, M. Godec and D. Steiner, *J. Mag. Mag. Mat.*, 133 (1994) 229

[17] M. Jenko, F. Vodopivec, H. J. Grabke, H. Viefhaus, B. Praček, M. Lucas, M. Godec, *Steel Research*, 65 (1994) 11, 500

[18] M. Jenko, H. Viefhaus, M. Lucas F. Vodopivec, M. Godec, D. Steiner Petrovič, M. Milun, T. Valla, *Metals, Alloys, Technologies*, 28 (1994) 4, 561-565

[19] M. Jenko, F. Vodopivec, H. Viefhaus, M. Godec, D. Steiner Petrovič, *Journal de Physique IV*, Colloque C7, 5, novembre 1995, C7-225-231

[20] R. Mast, H. J. Grabke, M. Jenko and M. Lukas, in print

[21] P. Ševc, J. Janovec, M. Lucas, H. J. Grabke, *Steel Research*, 66 (1995) 12, 537-542

[22] Rusenberg, H. Viefhaus, *Surf. Sci.*, 172 (1986) 615

[23] H. Viefhaus and M. Rüsenberg, *Surface Science*, 159 (1985) 1-23

[24] H. Viefhaus, *Analytica Chimica Acta*, 297 (1994) 43-53

[25] H. J. Grabke, *Kovine, zlitine, tehnologije*, (1993) 1-2, 9

[26] C. Lea, M. P. Seah, *Phil. Mag.*, 35 (1977) 1, 213

[27] E. D. Hondros, M. P. Seah, *Metal Trans.*, 8A (1977) 1363

[28] C. L. Briant, M. Ritter, *Acta metall.*, 32 (1984) 2031

[29] P. Gas, M. Guttman, J. Bernardini, *Acta metall.* 30 (1982) 1309

[30] K. Iwayama, K. Kuroki, Y. Yoshitomi, K. Homma and T. Wada: *J. Appl. Phys.*, 55 (1984) 2134

[31] V. Rüsenberg, H. Viefhaus, *Surf. Sci.*, 172 (1986) 615

[32] Beguinot and P. Lesbats, *Metalography*, 10 (1977) 115-119

[33] M. Godec, M. Jenko, F. Vodopivec, M. Ambrožič, Đ. Mandrino, L. Kosec, M. Lovrečič Saražin, *Kovine, zlitine, tehnologije*, 28 (1994) 1-2, 105-109

[34] W. Jager, H. J. Grabke, R. Möller, *4th International Conference*, Portorož, Jugoslavija, 1985

[35] H. De. Rugy and H. Viefhaus, *Surface Science*, 173 (1986) 418-438

[36] M. Godec, The influence of the segregated tin on the recrystalization behaviour of non oriented electrical steel sheet, PhD Thesis, University of Ljubljana, Ljubljana 1997

[37] D. Marton, J. Fine, *Optical Socoiety of America, Technical Digest*, 3 (1992) 146-148

[38] M. H. Mintz, P. Shukeer, J. Fine, *Surface Science Letters*, 238 (1990) L473-L477

Acknowledgement

The investigation was supported by the Ministry of Science and Technology of Slovenia, Contract No J2-7228-96.